

# The period-luminosity relations of red supergiants

Biwei Jiang<sup>1,2</sup> , Yi Ren<sup>3</sup>  and Ming Yang<sup>4</sup>

<sup>1</sup>Institute for Frontiers in Astronomy and Astrophysics, Beijing Normal University, Beijing 102206, China

email: [bjiang@bnu.edu.cn](mailto:bjiang@bnu.edu.cn)

<sup>2</sup>Department of Astronomy, Beijing Normal University, Beijing 100875, China

<sup>3</sup>College of Physics and Electronic Engineering, Qilu Normal University, Jinan 250200, China

<sup>4</sup>National Astronomical Observatories, Chinese Academy of Sciences, Beijing 100101, China

**Abstract.** Red supergiants (RSGs) are the brightest stars in the near-infrared. The existence of their period-luminosity relation (PLR) will be very helpful in determining cosmological distances. This review discusses the development in identification of RSGs, calculation of their light variation period, determination of the PLR, and the uncertainties associated. It is found that the PLR of RSGs exhibits the smallest scatter in the near-infrared, in particular within the  $P - M_K$  relation. The PLRs in the LMC, SMC, M31, and M33 show no obvious dependence on the galactic metallicity, which follows approximately the relation as  $M_K \approx -3.1 \log P - 1.9$ .

**Keywords.** red supergiant, period-luminosity relation, Magellanic Clouds, M31, M33

## 1. Introduction

Red supergiants (RSGs) are evolved Population I stars with helium-burning in the core. They are massive with a mass range between about 8–30  $M_\odot$ , but the lower and upper mass limits may vary depending on the metallicity and stellar models. With radii up to  $1000R_\odot$  or more, luminosities of RSGs can reach to  $10^5 L_\odot$ . Meanwhile, their effective temperature  $T_{\text{eff}}$  ranges from about 3500 K to 4500 K, which makes them the brightest stars in the near-infrared. For example, the brightest RSG can have an absolute magnitude in the  $K$  band of  $M_K \sim -12$  mag. Even at a cosmological distance of 1 Gpc (i.e.  $z \sim 0.25$ ), the apparent  $K$ -band magnitude would be  $m_K = 28$  mag, neglecting the extinction, which is still visible by the JWST. As a potential cosmological candle, the period-luminosity relation (PLR) of RSGs deserves investigation.

Pulsation is an important process with respect to the structure and evolution of RSGs, which is often considered to play a crucial role for driving the stellar wind (Yoon & Cantiello 2010). Through the wind, pulsation changes stellar structure, and consequently influences seriously the final fate of RSGs to be type II-P supernova or not, e.g., evolves bluewards to become blue supergiants/Wolf-Rayet stars or directly collapses to black hole (Kochanek et al. 2008; Ekström et al. 2012).

Early in 1942, Wilson & Merrill (1942) studied the PLR of a handful of RSGs in the Milky Way which were identified by spectroscopy. They concluded that there was an anti-correlation between the light variation period and luminosity. The mistake came mainly from the measurement of the absolute magnitude; the proper motion was used to derive the distance and then used to convert the apparent magnitude to the absolute magnitude. In addition to the distance uncertainty, they failed to correct for interstellar extinction,

when such extinction was very poorly understood at the early stage of discovery in 1930 (Trumpler 1930). Because RSGs are generally young stars with an age of about 8-20 Myr, they are supposedly located quite close to the Galactic plane where the extinction is very severe and inhomogeneous. The brightest RSGs may be the most distant and suffer the highest extinction so that the lack of extinction correction can lead to a large underestimation of their brightness. The problem of interstellar extinction has always been an obstacle in determining the PLR of RSGs in the Milky Way (and in other galaxies though to a much less extent).

By assuming that the variability of RSGs is due to radial pulsation, Stothers (1969) calculated the theoretical Q-values of variable RSGs in adiabatic equilibrium and compared with the observational ones. He found that, "With our adopted periods, no P-L or Period-spectrum relation emerges from the data". He suspected that some periods were incorrect and continued with "a suitable readjustment" of these periods, and then concluded that "pulsation seems to be suggested by ... (2) a period-luminosity relation.....". Taking  $\alpha$  Sco as an example, Stothers (1969) adjusted the observational period, 1733 days to 180 day with a Q-value of 0.06 day. However, modern studies derived its period to be  $1650 \pm 640$  day by Kiss et al. (2006), which confirmed the early observation.

What complicates the determination of the PLR of RSGs in the above works are mainly the ignorance of Galactic interstellar extinction and the complex variation of RSGs. The inhomogeneous extinction leads to the large uncertainty in distance and luminosity calculation. The light variation of RSGs very often contains some irregular components, which may be caused by convection, hot spot, high-order overtone mode, binary, etc. Consequently, the light curve may appear "irregular" and the determination of period becomes difficult and uncertain.

Most RSGs show some degree of variability. The typical amplitude of variation in the V band is about 1.0 mag, while in the near-infrared the amplitude is smaller, about 0.25 mag in the K band. According to the characteristics of light variation, the RSG variability is divided into three classes: irregular that is too complex to be delineated by any period, semi-regular with a short period (several hundred days), and the other with a long secondary period (LSP, with a period of thousand of days). Figure 1 shows the typical light curves of the three types.

## 2. The period-luminosity relation of red supergiants in the Magellanic Clouds

The success in determining the PLR of RSGs came when astronomers turned their observations to nearby galaxies, i.e. the Large and Small Magellanic Clouds (LMC and SMC), which is very like the case of the Cepheid variables. The same distance in a nearby galaxy means that the relative absolute luminosity can be expressed by the relative apparent one, which makes the PLR more precise.

Glass (1979) observed 38 late-type supergiants in the MCs in the near-infrared *JHKL* bands. He mentioned the usefulness of RSGs as distance indicators. Afterwards, Feast et al. (1980) used 24 red supergiants in the LMC to determine the PLR. They derived the bolometric magnitude from the *JHKL* photometry by using a kind of blackbody spectral energy distribution (SED) fitting. Based on the result, they justified the existence of the PLR of red supergiants. Their PLR has the form of  $M_{\text{bol}} = -8.6 \log P + 16.4$ , which roughly coincides with the semi-theoretical relation.

In addition to the same distance, the RSGs in the LMC are not located deep inside the interstellar dust, which reduces the extinction effect. Moreover, the near-infrared extinction is only about a tenth of the visual bands (e.g., the V-band), further reducing the effect of interstellar extinction. One year later, Catchpole & Feast (1981) published the PLR of 22 RSGs in the SMC and concluded that "the SMC red supergiant variables fit

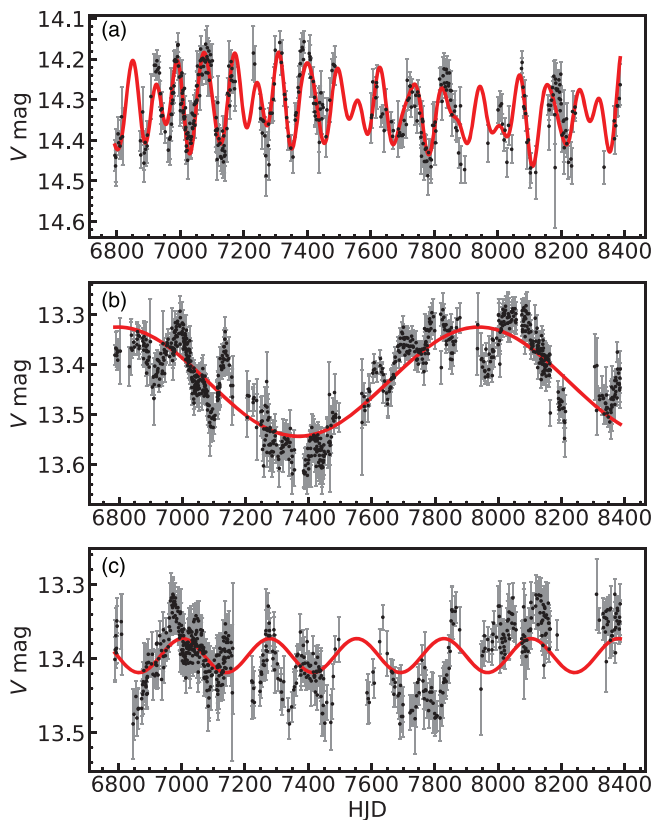


**Figure 1.** Three types of light variation of red supergiants. Top, middle, and bottom panels show a semi-regular RSG, a RSG with long secondary period, and a RSG with irregular variation, respectively. The red lines show the fitting by periodic functions.

the P-L relation previously derived for the LMC stars". This may be the first suggestion that the PLR of RSGs in the near-infrared is independent of metallicity, since the metallicity of the SMC and LMC differs by a factor of two. Later on, Wood et al. (1983) confirmed the PLR of RSGs in the MCs.

Typically, RSGs have periods about several hundred days with a semi-regular and complex variability. Consequently, a sufficiently long baseline is needed for studying their PLR, which is facilitated by the large-scale time-domain surveys developed quickly since 1990s with the advancement of detectors and driven by various sciences. In order to search for the Massive Halo Compact Objects (MACHOs), which was the candidates for dark matter, several projects like MACHO, OGLE, EROS, etc., were conducted to detect variable objects in densely populated star fields, such as the Galactic bulge and the Magellanic Clouds. In recent decades, more long-term surveys have been developed to monitor supernovae explosions which are important to cosmology. For example, the ASAS and its successor ASAS-SN are survey projects dedicated to relatively bright stars in the whole sky with small telescopes. PTF and its successor ZTF can detect objects as faint as 20 mag in the *R*- and *g*-band. These surveys naturally monitor the light variation of RSGs in the field, which greatly increases the sample size of RSGs for which the period can be determined.

Yang & Jiang (2011) and Yang & Jiang (2012) analyzed the light variation of 191 and 126 RSGs in LMC and SMC, respectively. With the nearly a decade long time-series photometric observation by ASAS and MACHO, they calculated the characteristics of light

variation to classify the RSGs into three variable classes: irregular, semi-regular, and LSP. For the semi-regular and the LSP variable with distinguishable short period, they determined the PLR in the visual and near-infrared bands which include the 2MASS/ $JHK_S$ , Spitzer/IRAC1-4 and Spitzer/MIPS24. It is found that the PLR is tight in the infrared bands such as the 2MASS  $JHK_S$  bands and the Spitzer/IRAC bands. Meanwhile, the PLR is relatively sparse in the  $V$  band because the visual extinction is larger with larger dispersion than in the infrared bands. There is also relatively large scatter in the MIPS24 band possibly due to the influence of circumstellar dust emission of RSGs.

### 3. The period-luminosity relation of red supergiants in M31 and M33

The first application of the PLR of RSGs in M33 was by Kinman et al. (1987). They used the PLR derived from the LMC RSGs to calculate the distance according to the periods and apparent  $K$ -band magnitudes of RSGs in M33. The derived distance modulus was 24.64 which agrees very well with modern results. This successful application indicates that the PLRs of RSGs in M33 and LMC are consistent with each other.

Soraisam et al. (2018) analyzed the light variation of 255 spectroscopically identified RSGs in M31 based on the PTF data and found that 63 of them showed significant pulsation periods. They derived the PLR which was consistent with those in LMC, SMC and M33 over various metallicities.

Ren et al. (2019) used the time-series data from the iPTF survey spanning nearly 2000 days. For 84 and 56 RSGs classified as semi-regular variables in M33 and M31, respectively, they determined the periods with four popularly used methods, i.e. phase dispersion minimization (PDM), Generalized Lomb-Scargle Periodogram (GLS), Weighted Wavelet Z-transform (WWZ), and Discrete Fourier Transform (DFT). A period was accepted only when the periods derived by at least two methods were consistent with each other. The uncertainty of period was estimated to be about  $\sim 10\%$  of the period. Such accuracy cannot compete with other types of regular variables like Cepheids, RR Lyraes or Miras. Nevertheless, the PL relations based on the derived periods are tight in the near-infrared, i.e. in the  $JHK_S$  bands and the Spitzer/IRAC1 and IRAC2, which is the same as the case of the MCs.

## 4. Discussion

### 4.1. The sample, complete or incomplete

The early identification of RSGs in an external galaxy relied on spectroscopy of high-luminosity red targets, which showed the spectral features of a RSG (e.g., the broad absorption bands of TiO) and the radial velocity of an extragalactic object. The RSGs in the Magellanic Clouds were mostly identified in this way. Unfortunately, spectroscopy is time-consuming and applicable only to apparently bright objects, i.e. the RSGs in the MCs or the brightest RSGs in M31 and M33 etc. Spectroscopic identification may suffer severe contamination of red dwarfs and giants in the Milky Way, as well as asymptotic giant branch stars (AGBs) in the target galaxy. Later, Massey (1998) developed a method to identify extragalactic RSGs by photometry. They used the  $B - V/V - R$  color-color diagram (in Johnson system) to distinguish extragalactic supergiants from foreground dwarf stars on the basis that the  $B$  band covers many metallic lines so that  $B - V$  is sensitive to stellar surface gravity in addition to effective temperature. In comparison with spectroscopy, photometry is much more efficient and able to detect much fainter RSGs. By using this method, they identified 437 and 776 RSG candidates in M31 and M33 respectively, and the later spectroscopic observations of some of these confirmed that the radial velocities and spectral types are consistent with RSGs. In comparison with a few tens of RSGs in previous studies, this sample size was increased by an order

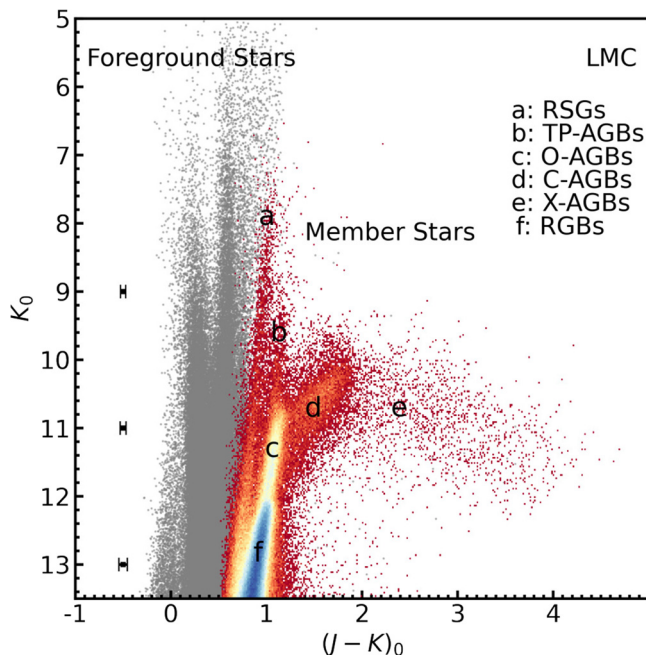


**Figure 2.**  $(J - K)_0/K_0$  of member stars (color density map) in LMC. Removed foreground stars are gray dots. The error bars show the mean error of  $J - K$  at different  $K$  magnitudes. Member stars include RSGs, thermally pulsing AGBs (TP-AGBs), oxygen-rich AGBs (O-AGBs), carbon-rich AGBs (C-AGBs), extreme AGBs (X-AGBs), and red giant branch stars (RGBs).

of magnitude. It was based on this sample that Ren et al. (2019) analyzed the PLR of RSGs in M31 and M33 in the near-infrared bands.

The photometric method is much more efficient than spectroscopy. However, such an optical color-color diagram is not practical at the faint end because the difference between red supergiant and dwarf stars is small in  $B - V$ . A photometric accuracy of about 0.01 mag is needed for clear discrimination. Moreover, the interstellar extinction mixes up the two classes. Finally, the modern filter sets have different effective wavelengths and coverages from the Johnson system.

#### 4.1.1. The Magellanic Clouds

The Gaia space telescope brings about astrometric information to identify member stars in addition to providing astrophysical information. Yang et al. (2019) identified the SMC members by using stellar proper motions and parallaxes in the *Gaia/DR2* datasets. The stars within a  $5\sigma$  range of the proper motion distributions are taken as the candidates for membership. Together with other information such as parallax, radial velocity and the locations in the color-magnitude diagram, they identified 1,405 red supergiants in SMC. In more or less the same way, they further identified 2,974 RSGs in LMC (Yang et al. 2021). On this basis, Ren et al. (2021b) adopted the *Gaia/DR3* datasets which included many more member stars of the MCs than *Gaia/DR2* and refined the method by using the near-infrared color-color diagram (to be described below) and correcting the interstellar extinction. They finally identified 4,823 and 2,138 RSGs in LMC and SMC, respectively. Figure 2 displays the extinction corrected  $(J - K)_0/K_0$  diagram of LMC stars identified in this way.

Based on new samples of RSGs in the LMC and SMC and time-series data from the Optical Gravitational Lensing Experiment (OGLE; Udalski et al. 2015; Soszyński et al. 2015) and the All-Sky Automated Survey for SuperNovae (ASAS-SN; Shappee et al. 2014; Kochanek et al. 2017; Jayasinghe et al. 2020), we investigated the PLR of RSGs in the LMC and SMC. The overview and processing of time-series data are as follows:

(1) Overview of Time-Series Data. The ASAS-SN, which contains 20 telescopes worldwide, observes variable objects in the LMC and SMC at a cadence of 4-5 days spanning  $\sim 2000$  days with magnitude limits of  $\sim 18$  at  $g$  band and  $\sim 17$  at  $V$  band. The OGLE is a long-term photometric survey focused on variables, which observes the brightness of sources in the SMC and LMC at a cadence of 1-2 days and accumulates time-series data over 10 years.

(2) Removal of Outliers. For each light curve, the first quartile ( $Q_1$ ), the third quartile ( $Q_3$ ), and the corresponding interquartile range (IQR;  $IQR = Q_3 - Q_1$ ) are calculated from the brightness distribution of a light curve. The photometry points beyond the range (i.e.  $< Q_1 - 1.5 \times IQR$  or  $> Q_3 + 1.5 \times IQR$ ) are regarded as outliers.

(3) Removal of White-Noise Sequences. In this work, ASAS-SN performed forced photometry at the coordinates of the RSGs. This photometry strategy still generates light curves for some sources which are fainter than the detection threshold. So we perform white noise test on light curves. Specifically, if over 95% of the autocorrelation functions (ACFs) of a light curve lie in the region expected for a white-noise process, this light curve is regarded as white-noise and removed.

After time-series data preprocessing, for RSGs in the LMC, there are 2665, 2123, and 2656 light curves in the  $g$ ,  $V$ , and  $I$  bands, respectively. For RSGs in the SMC, there are 886, 452, and 1337 light curves in the  $g$ ,  $V$ , and  $I$  bands, respectively. There are 4471 and 1924 RSGs with at least one band photometry in the LMC and SMC, respectively.

Then the Lomb-Scargle (LS) periodogram method is introduced to determine the periods of RSGs. The periods of all three bands are determined. If one source has been observed at  $g$ ,  $V$ , and  $I$  bands, we prefer the period of the  $V$  band, followed by the  $g$  band, and finally the  $I$  band. Because compared with the  $I$  band, the light curve has a higher amplitude in the  $V$  band, and there are more measurements than in the  $g$  band. To further eliminate the impact of fake periods determined by the LS method, we calculate the Pearson correlation coefficient ( $R$ ) between the light curves of different bands (i.e.  $R_{gV}$ ,  $R_{gI}$ , and  $R_{VI}$ ). The RSGs in the LMC (SMC) used to obtain the PLR are required to have at least one Pearson correlation coefficient greater than 0.6 (0.3). In addition, RSGs with period greater than 1000 days are excluded from further analysis.

Due to the increase in the sample size, we can simultaneously observe RSGs in different pulsation modes in the PLR diagram as shown in Figure 3. Therefore, it is necessary to first classify the pulsation modes of RSGs, and we select three lines to fit three different pulsation modes. The slope of the three lines is selected as Yang & Jiang (2011) (i.e.  $-3.75$ ) and fixed, and the three intercepts are free parameters. During the fitting process, the point is classified to one line to which Euclidean distance from the observation point is smallest. Finally, optimize the overall  $\chi^2$  to obtain the intercept of the three lines, and obtain the classification of the RSGs pulsation modes as shown in Figure 3.

For RSGs in fundamental pulsation mode, we calculate their multi-band PLRs, the  $V$  band brightness is taken from ASAS-SN, while the  $JHK_S$  bands brightness comes from 2MASS. The multi-band PLRs are presented in Figure 4.

#### 4.1.2. The M31 and M33

The application of the Gaia measurements to the MCs greatly increased the sample size of RSGs by about one order of magnitude from previous samples. On the other

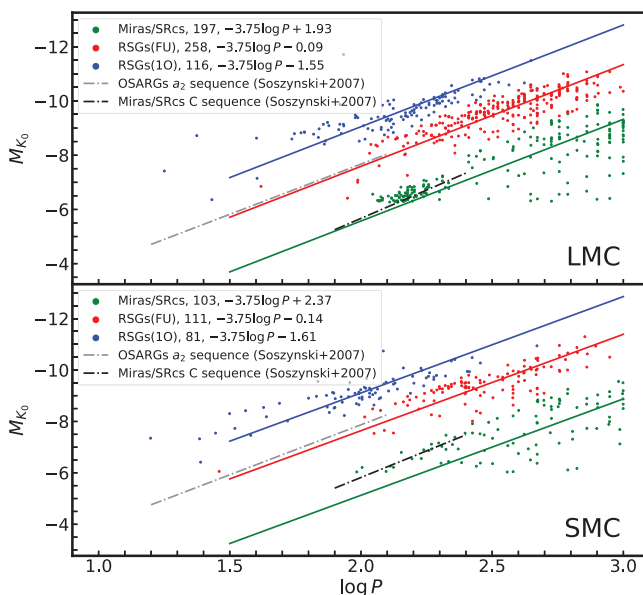


**Figure 3.** The PLR of the new samples of RSGs in the MCs. The distance moduli of LMC and SMC are 18.26 and 18.72, respectively (Ren et al. 2021b). Blue dots are RSGs in the first overtone pulsation mode. Red dots are RSGs pulsating in the fundamental mode, gray dash-dotted line is OGLE Small Amplitude Red Giants (OSARGs)  $a_2$  PLR sequence (Soszyński et al. 2007) for comparison. Green sources are Mira variables and RSGs with long secondary period, black dash-dotted line is Miras/SRcs C PLR sequence (Soszyński et al. 2007) for comparison.

hand, this also indicates that the RSG samples of 437 and 776 objects (Ren et al. 2019) are far from complete in M31 and M33 and need to be replenished. With a distance modulus (d.m.) of about 24.5 mag, M31 and M33 are much further than the MCs at a d.m. of about 19 mag. Consequently, Gaia measured only few percent of the member stars. The identification by proper motion or parallax of member stars then becomes very inefficient. Ren et al. (2021a) developed a new method based on the near-infrared color-color diagram, i.e.  $J - H/H - K$ . In methodology, this is similar to the  $B - V/V - R$  method. This near-infrared color-color diagram uses the sensitivity of the  $H$ -band, that includes many molecular bands, to surface gravity to distinguish the red (super)giants from the foreground dwarfs. As an example, the  $J - H/H - K$  diagram of point sources is displayed in Figure 5 for M33, where the intrinsic color indexes of dwarfs, giants and supergiants are plotted for reference (Bessell & Brett 1988). Obviously, the foreground dwarf stars constitute an inverse “V”-shaped branch, while the member red giants, AGBs, and RSGs are well above the dwarf branch. After removing the foreground stars, the color-magnitude diagram becomes very clean where the RSGs can be easily recognized by their high brightness and relatively bluer colors than AGBs. Ren et al. (2021a) identified 5,498 and 3,055 RSGs in M31 and M33 respectively by this method. The spatial distribution of RSGs in M31 and M33 is presented in Figure 6, which coincide with the ring in M31 and spiral arms in M33 as expected for massive stars. Due to the photometric error in the crowded field, the sample may suffer an uncertainty of about 10% for M33 and 20% for M31, but this still is the most complete and pure sample of RSGs in these two galaxies.

#### 4.2. Universality

Whether the PLR of RSGs is universal or not is very important for its application to cosmology. It is also important to the physics of RSGs. The first sign of universality

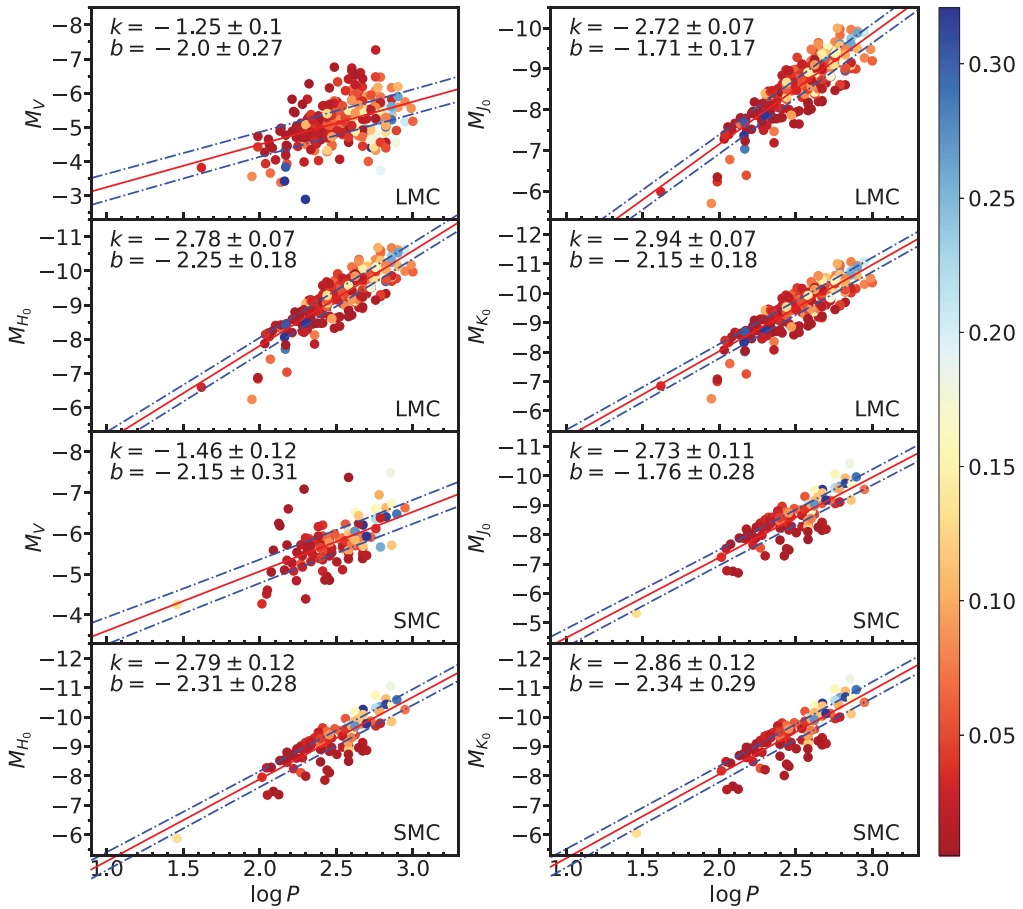


**Figure 4.** PLR in the  $VJHK$  bands for RSGs in fundamental pulsation mode in MCs. The red solid line is a linear fit between the multi-band absolute magnitude and the period. The blue dash-dotted lines indicate the prediction interval at 0.35 significance level. The color of dots decodes the  $V$  band amplitude in accord with the color bar (in the unit of magnitude).

appeared when [Catchpole & Feast \(1981\)](#) published the PLR of 22 RSGs in the SMC and concluded that “the SMC red supergiant variables fit the P-L relation previously derived for the LMC”, since the metallicity of the SMC is only about half that of the LMC. Later confirmation came from [Pierce et al. \(2000\)](#) who studied the RSGs in the Per OB1 association, the LMC and M33. They estimated the distances to the Per OB1 and M33 by using the PLR of RSGs in the LMC, and obtained results consistent with other methods. This indicated that the PLR derived from the LMC can be applied to the RSGs in much more metal-rich environments.

[Ren et al. \(2019\)](#) compared the  $\log P - M_K$  relation of RSGs in the SMC, the LMC, the Milky Way, M33, and M31. They found that the PLR obeyed similar law in these galaxies except the Milky Way, i.e. the slopes are all consistent within the uncertainty. Specifically,  $M_{K_S} \sim -3.1 \log P - 1.9$ , with a dispersion of about 0.2 mag. The PLR of RSGs in the Milky Way will be more uncertain due to the large dispersion of the estimated distances caused by heterogeneous interstellar extinction. This suggests that the  $\log P - M_K$  relations in the  $K$  band is universal in these nearby galaxies. In that sense, RSGs can be used as a distance indicator. It must be emphasized that, the universality of PLR in the infrared bands does not imply the PLR is universal in the optical bands.



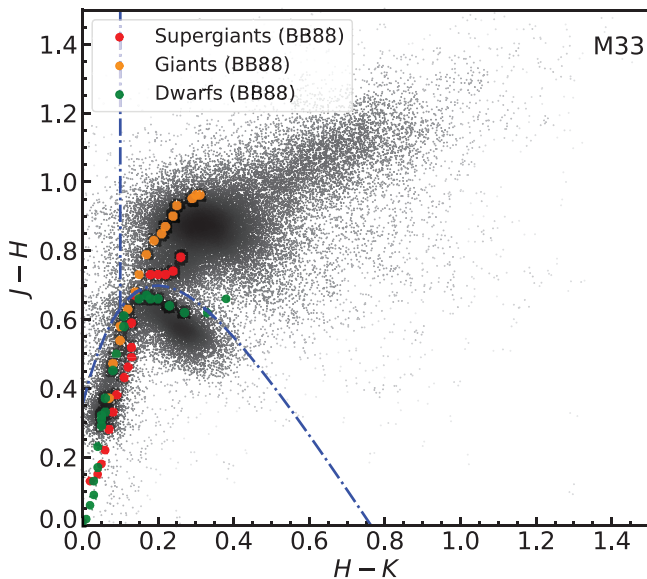


**Figure 5.** The NIR CCD of the point sources in the field of M33. The blue dash-dotted line is the dividing line between foreground dwarfs and member (super)giants. For comparison, the intrinsic color indexes of dwarfs (green dots), giants (yellow dots), and supergiants (red dots) are taken from [Bessell & Brett \(1988, BB88 for short\)](#).

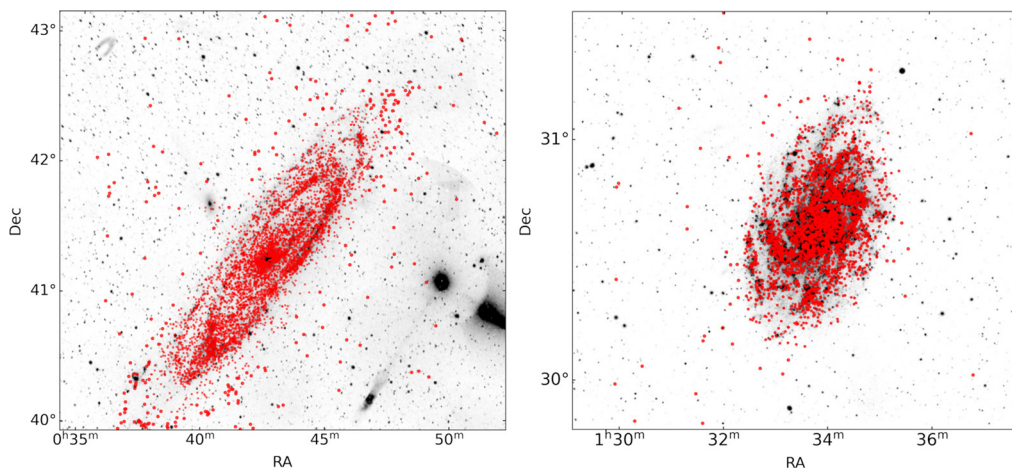


**Figure 6.** Spatial distribution of RSGs in M31 (left panel) and M33 (right panel). The background is the GALEX ultraviolet observation.

[Ramírez & Meléndez \(2005\)](#) pointed out that metallicity has much weaker influence on stellar infrared colors than optical color. Moreover, the much higher visual extinction with larger dispersion makes the PLR in the optical band very scattered, so that the uncertainty of the  $\log P - M_V$  relation is too large to discuss its universality.

Figure 7 shows the PLR in  $K$  band. The PLR of RSGs in M31 is derived using the sample from [Ren et al. \(2021a\)](#) and time-series data from ZTF DR16. The periods of RSGs in M33 are taken from [Ren et al. \(2019\)](#), while the  $K_0$  magnitudes come from [Ren et al. \(2021b\)](#).

As can be seen from Figure 7, the PLRs of RSGs in the SMC, LMC, and M31 are consistent within the uncertainty. The slope of the PLR of RSGs in M33 is rather large.

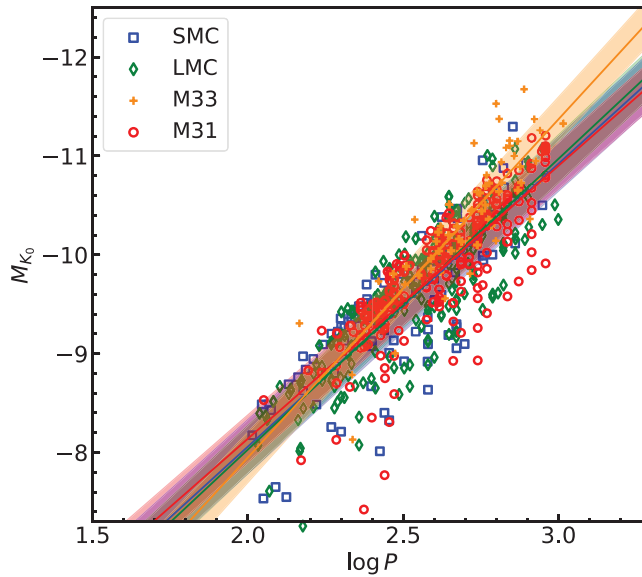


**Figure 7.** PLRs in  $K$  band for RSGs in SMC, LMC, M33, and M31, where only the fundamental mode period is adopted. The distance moduli of SMC, LMC, M33, and M31 are taken from [Ren et al. \(2021b\)](#). The  $K$  band magnitudes are extinction corrected.

However, the sample of RSGs in M33 is incomplete, the PLR of RSGs in M33 need to be recalibrated.

#### 4.3. Pulsation mode

In the theoretical calculation of [Stothers \(1969\)](#), he assumed the fundamental mode of radial pulsation for red supergiants. [Li & Gong \(1994\)](#) made a comprehensive study on the pulsation of RSGs in the LMC with a linear nonadiabatic analysis. They found that the fundamental mode, and sometimes the first overtone mode, were unstable and that the observed PLR could be well understood by the fundamental-mode hypothesis. [Guo & Li \(2002\)](#) made further linear non-adiabatic calculation of RSGs at different metallicity and predicted the PLR for the fundamental, first-overtone and second-overtone modes.

[Yang & Jiang \(2011\)](#) and [Yang & Jiang \(2012\)](#) compared the PLR derived from the observational data with the theoretical calculation of [Guo & Li \(2002\)](#). They indicated that the majority of RSGs in LMC and SMC might pulsate in the first-overtone mode, while the Galactic RSGs mainly pulsate in the fundamental mode. On the other hand, [Ren et al. \(2019\)](#) identified the pulsation mode of RSGs in M31 and M33 to be mainly in the fundamental mode, also by comparing with the theoretical predictions of [Guo & Li \(2002\)](#). They further studied the ratio of fundamental-to-first overtone mode with respect to the metallicities for the SMC, the LMC, the Milky Way, M33, and M31. It is found that the ratio of RSGs pulsating in the fundamental mode to the first overtone mode increases with the metallicity. This is explained by the metallicity effect on convection. Convection becomes stronger with increasing metallicity, which suppresses the first-overtone mode in the shallower atmosphere than the fundamental mode. Such phenomena were later confirmed by Cepheids. [Zhang et al. \(2022\)](#) calculated the Cepheids ratio of  $FU/(FU+10)$  to be 0.59, 0.60, 0.69, 0.83, and 0.85 for the SMC, the LMC, the Milky Way, M33, and M31, respectively, in order of metallicity, which confirms that the ratio of  $FU/(FU+10)$  increases with metallicity. It should be mentioned that [Soraisam et al. \(2018\)](#) compared their observational results of RSGs in M31 with the MESA model and concluded that

the bulk of the pulsating RSGs in their sample are consistent with the fundamental mode. Thus, in spite of different theoretical models and observational analysis, the same conclusion is drawn that the fundamental mode dominates in the relatively metal-rich galaxies.

It can be concluded that RSGs pulsate both in the fundamental and first-overtone mode, while the second-overtone mode has not yet been reported. Although the PLR in the near-infrared appears to be independent of metallicity, the pulsation mode indeed depends on metallicity.

#### 4.4. Irregular light variation of RSGs

The period determination of RSGs has always been a troublesome thing. Although quite a few methods are developed to solve the periodicity of light variation, the uncertainty of period can still be a few tens of days. This is due to the complex irregular components in the light curves of RSGs.

The irregular variation actually presents in all three variable types of RSG. The widely accepted mechanism for irregular variation is the large convection cells in the photosphere, since RSGs have a convective envelope due to the high opacity in the low-temperature extended atmosphere. Studies suggested that the surface of RSGs should be dominated by a few large convective cells (Schwarzschild 1975), which was later confirmed by the 3D simulation (Freytag et al. 2002).

Ren & Jiang (2020) investigated the characteristic time scale and amplitude of irregular variation of RSGs in the SMC, the LMC and M31 based on the granulation model. With the timeseries data from the ASAS-SN and iPTF survey, it is found that the granulations in most of the RSGs evolve at a timescale of several days to a year with a characteristic amplitude of 10 to 1000 mmag. The comparison between the SMC, the LMC and M31 indicates that the timescale and amplitude of granulation seem to increase with metallicity.

The irregular variation and periodic variation are generally tangled together. The PLR could be more accurate if the irregular component can be removed or considered together.

In addition, the binary fraction of unevolved massive stars is thought to be 70%-100% (Sana et al. 2012), while studies show that the binary fraction of RSGs is about 20% (Neugent et al. 2020; Patrick et al. 2022). The RSG in a binary system would present another highly different light variation component. This surely makes the light curve more complicated.

#### 4.5. In the Galaxy

The PLR of RSGs in our Galaxy suffers large uncertainty. The difficulty within the Galaxy is caused by the interstellar extinction as exhibited in the very first work by Stothers (1969). Because RSGs are mostly located in the Galactic plane, the very serious extinction leads to non-detection of RSGs at relatively large distance, and to uncertainty in the measurement of brightness and temperature. Thus the identification of RSGs in the Milky Way is difficult and uncertain. Except in a few nearby open clusters, only a small number of RSGs are identified. In a recent work by Messineo & Brown (2019), they collected 889 nearby candidate RSGs with reliable parallaxes from Gaia/DR2. With estimation of stellar luminosity and effective temperature, only 43 of them are thought to be highly-probably red supergiants with  $M_{\text{bol}} < -7.1$  mag. In comparison with the number of RSGs identified in M31 and M33 which are spiral galaxy like our own, this number is only about one percent of the expected. Gehrz (1989) also predicted  $\sim 5,000$  RSGs in our Galaxy based on the stellar distribution model.

Chatys et al. (2019) analyzed the  $\log P - M_K$  relation of 48 RSGs in the Galaxy with the distances from Gaia/DR2. Still, the dispersion is large though the distances may be more accurate than previous measurements. They found that the  $\log P - M_K$  relation agreed well with that in the LMC or M33 (Yang & Jiang 2011; Soraisam et al. 2018). A better determination of the RSG PLR in our galaxy can be achieved in a few aspects. A large and more complete sample will reduce the dispersion statistically. A more accurate calculation of interstellar extinction will reduce the error of luminosity. Observation in the near-infrared will detect more distant RSGs as well.

## 5. Summary

Red supergiants are the near-infrared brightest stars and potential cosmological distance indicators. Their period-luminosity relation has been studied in the Galactic associations and fields, the Magellanic Clouds, M31 and M33. With the large-scale long-term surveys, many more RSGs are identified and their periodicities are measured. It is suggested by various works that the period- $M_K$  relation presents no obvious difference in these systems, which may be attributed to the small influence of metallicity on their infrared brightness and small extinction in the infrared. The dispersion may be further reduced with better determination of periods by taking the irregular variation and binary effect into account. On the other hand, the sample of RSGs in our Galaxy is far from complete, and the measurement of the period-luminosity relation needs more sources and more accurate measurement of distance and extinction.

This work is supported by the NSFC project 12133002, National Key R&D Program of China No. 2019YFA0405503, and CMS-CSST-2021-A09.

## References

- Bessell, M. S. & Brett, J. M. 1988, *PASP*, 100, 1134  
 Bouvier, J. 2013, EAS Publications Series, 143  
 Catchpole, R. M. & Feast, M. W. 1981, *MNRAS*, 197, 385  
 Chatys, Filip W., Bedding, Timothy R., Murphy, S. et al. 2019, *MNRAS*, 487, 4832  
 Collier Cameron, A. 1999, Solar and Stellar Activity: Similarities and Differences, 146  
 Donati, J.-F., Brown, S. F., Semel, M., et al. 1992, *A&A*, 265, 682  
 Ekström, S., Georgy, C., Eggenberger, P., et al. 2012, *A&A*, 537, A146.  
 Feast, M. W., Catchpole, R. M., Carter, B. S, et al. 1980, *MNRAS*, 193, 377  
 Freytag, B., Steffen, M. & Dorch, B. 2002, *AN*, 323, 213  
 Gehrz, R. 1989, *IAUS*, 135, 445  
 Glass, I. S. 1979, *MNRAS*, 186, 317  
 Guo, J. H. & Li, Y. 2002, *A&A*, 565, 559  
 Kinman, T. D., Mould, J. R. & Wood, P. R. 1987, *AJ*, 93, 833  
 Kiss, L. L., Szabó, Gy. M., Bedding, T. R. 2006, *MNRAS*, 372, 1721  
 Kochanek, C. S., Beacom, J. F., Kistler, M. D., et al. 2008, *ApJ*, 684, 1336.  
 Li, Y. & Gong, Z. G. 1994, *A&A*, 289, 449  
 Massey, P. 1998, *ApJ*, 501, 153.  
 Massey, Philip, Olsen, K. A. G., Hodge, Paul W. et al. 2006, *AJ*, 131, 2478  
 Messineo, M. & Brown, A. G. A. 2019, *AJ*, 158, 20  
 Neugent, Kathryn F., Levesque, Emily M., Massey, Philip et al. 2020, *ApJ*, 900, 118  
 Patrick, L. R., Thilker, D., Lennon, D. J. et al. 2022, *MNRAS*, 513, 5847  
 Pierce, M. J., Jurcevic, J. S. & Crabtree, D. 2000, *MNRAS*, 313, 271  
 Ramírez, Iván & Meléndez, Jorge 2005, *ApJ*, 626, 465  
 Ren, Yi & Jiang, Biwei 2020, *ApJ*, 898, 24  
 Ren, Yi, Jiang, Biwei, Yang, Ming et al. 2019, *ApJS*, 241, 35  
 Ren, Yi, Jiang, Biwei, Yang, Ming et al. 2021a, *ApJ*, 907, 18  
 Ren, Yi, Jiang, Biwei, Yang, Ming et al. 2021b, *ApJ*, 923, 232

- Sana, H., de Mink, S. E., de Koter, A., et al. 2012, *Science*, 337, 444
- Schwarzschild, M. 1975, *ApJ*, 195, 137
- Soraisam, Monika D., Bildsten, Lars, Drout, Maria R. et al. 2018, *ApJ*, 859, 73
- Stothers, Richard 1969, *ApJ*, 156, 541
- Trumpler, Robert Julius 1930, *Lick Observatory Bulletin*, 420, 154
- Yoon, S., & Cantiello, M. 2010, *ApJ*, 717, 62
- Wilson, Ralph E. and Merrill, Paul W. 1942, *ApJ*, 95, 248
- Wood, P. R., Bessell, M. S. & Fox, M. W. 1983, *ApJ*, 272, 99
- Yang, Ming & Jiang, B. W. 2011, *ApJ*, 727, 53
- Yang, Ming & Jiang, B. W. 2012, *ApJ*, 754, 35
- Yang, Ming, Bonanos, Alceste Z., & Jiang, Biwei et al. 2019, *A&A*, 629, 91
- Yang, Ming, Bonanos, Alceste Z., & Jiang, Biwei et al. 2021, *A&A*, 646, 141
- Zhang, Zehao, Jiang, Biwei, Ren, Yi et al. 2022, *ApJ*, 928, 139
- Bouvier, J. 2013, *EAS Publications Series*, 143
- Collier Cameron, A. 1999, *Solar and Stellar Activity: Similarities and Differences*, 146
- Donati, J.-F., Brown, S. F., Semel, M., et al. 1992, *A&A*, 265, 682
- Shappee, B. J., Prieto, J. L., Grupe, D., et al. 2014, *ApJ*, 788, 48
- Kochanek, C. S., Shappee, B. J., Stanek, K. Z., et al. 2017, *PASP*, 129, 104502
- Jayasinghe, T., Stanek, K. Z., Kochanek, C. S., et al. 2020, *MNRAS*, 491, 13
- Udalski, A., Szymański, M. K., & Szymański, G. 2015, *AcA*, 65, 1
- Soszyński, I., Udalski, A., Szymański, M. K., et al. 2015, *AcA*, 65, 297
- Soszyński, I., Dziembowski, W. A., Udalski, A., et al. 2007, *AcA*, 57, 201

## Discussion

**Question (Whitelock):** I suspect that in your colour-magnitude diagram those objects that you described as thermally pulsing AGB stars are actually hot bottom burning AGB stars. That's not directly relevant to the red supergiants, but I think that's what is going on.

**Answer:** Maybe yes. We here only plotted the checks from the models. They are consistent with TP-AGB branch of stellar models. So that's why we assigned them TP-AGB stars.

**Question (Whitelock):** Can you say anything about very long secondary periods in supergiant stars?

**Answer:** That's a difficult question, there are many models about the long secondary period. I don't think any of these explanations is perfect, like binary or spot or whatever. One of our collaborators [Yi Ren] is very interested in this topic. We will see if we will have any new ideas on this.

**Question (Baruch):** On an early slide you showed some distances; you tried to generate distances and compared with Gaia. Do you get anything by giving a standard error from the Gaia measurements? Does that help? The SHOES group worked out those 24 microarcseconds, and if they took that away from the Gaia measurements they got really good answers. Can you do the same with your supergiants?

**Answer:** I have no idea actually now how to compare with this one. SHOES is for much distant galaxies while we are working on the Local Group Galaxies. Well, we derived the distance modulus for these galaxies, but based on the tip of the RGB population, so it has nothing to do with red supergiants.

**Question (Kervella):** I just wanted to ask if you tried (or maybe you didn't) the subtraction of the infrared excess that may be visible in the spectral energy distribution, to construct a dust-free period-luminosity relation with circumstellar emission removed?

**Answer:** This is a difficult problem, because the interstellar extinction and circumstellar extinction are actually mixed together. We do have a work to derive the mass-loss rate from the SED of red supergiants (Wang et al, 2021ApJ...912..112W). And then, if we increase the interstellar extinction, the mass-loss rate becomes smaller for sure, because the circumstellar extinction becomes smaller. But we did not decompose these two components. We just have to assume that the interstellar extinction derived in other ways independently are correct.